

# Microtubule-severing protein Katanin p60 ATPase-containing subunit A-like 1 is involved in pole-based spindle organization during mouse oocyte meiosis

LEI-LEI GAO<sup>1</sup>, FEI XU<sup>2</sup>, ZHEN JIN<sup>3</sup>, XIAO-YAN YING<sup>4</sup> and JIN-WEI LIU<sup>1</sup>

<sup>1</sup>Department of Gynecology, Zhejiang Provincial People's Hospital, People's Hospital of Hangzhou Medical College, Hangzhou, Zhejiang 310014; <sup>2</sup>Department of Gynecology, The Affiliated Hospital of Hangzhou Normal University, Hangzhou, Zhejiang 310015; <sup>3</sup>Reproductive Genetic Center, Suzhou Municipal Hospital, Suzhou Hospital of Nanjing, Nanjing, Jiangsu 215000; <sup>4</sup>Department of Gynecology, The Second Affiliated Hospital, Nanjing Medical University, Nanjing, Jiangsu 210011, P.R. China

Received December 15, 2018; Accepted May 31, 2019

DOI: 10.3892/mmr.2019.10605

**Abstract.** Microtubule-severing proteins (MTSPs) are a group of microtubule-associated proteins essential for multiple microtubule-related processes, including mitosis and meiosis. Katanin p60 ATPase-containing subunit A-like 1 (p60 katanin-like 1) is an MTSP that maintains the density of spindle microtubules at the poles in mitotic cells; however, to date, there have been no studies about its role in female meiosis. Using *in vitro*-matured (IVM) oocytes as a model, it was first revealed that p60 katanin-like 1 was predominant in the ovaries and oocytes, indicating its essential roles in oocyte meiosis. It was also revealed that p60 katanin-like 1 was concentrated at the spindle poles and co-localized and interacted with  $\gamma$ -tubulin, indicating that it may be involved in pole organization. Next, specific siRNA was used to deplete p60 katanin-like 1; the spindle organization was severely disrupted and characterized by an abnormal width:length ratio, multipolarity and extra aster microtubules out of the main spindles. Finally, it was determined that p60 katanin-like 1 knockdown retarded oocyte meiosis, reduced fertilization, and caused abnormal mitochondrial distribution. Collectively, these results indicated that p60 katanin-like 1 is essential for oocyte meiosis by ensuring the integrity of the spindle poles.

## Introduction

The microtubule cytoskeleton is essential for almost all cellular activities. Microtubules themselves are the main

components of important structures, such as spindles, axons and centrosomes, and mutations in tubulin-encoding genes cause severe human diseases, with their common cause being severe defects in microtubule organization (1-3). A key feature of the microtubule, upon which all its functions rely, is its dynamicity. For example, during interphase or each stage of mitosis in somatic cells, microtubules remain highly dynamic (growth, shrinkage, pause, catastrophe) at either or both ends to achieve diverse processes, such as vesicle and organelle transport, chromosome segregation, centrosome orientation and protein turnover (4-6). The dynamicity of microtubules is primarily determined by the cooperation of different families of microtubule-associated proteins (MAPs), thus, mutations or abnormalities of these MAPs are also the primary cause of certain severe human diseases (7-9). Among the various MAPs, microtubule-severing proteins (MTSPs), a meiotic subfamily of the AAA superfamily (containing ATP-associated proteins with diverse cellular activities), are crucial for microtubule (MT) dynamicity (10,11). MTSPs primarily use their microtubule-severing activities to sever MTs near their plus or minus ends to remove the protective caps, thereby exposing the free ends to MT polymerizer or depolymerizer (12-15). Another proposed major function of MTSPs is 'nucleating', which entails severing a long microtubule into multiple short segments so that each short part can polymerize into a new long microtubule to promote efficient MT organization (16). Notably, the mutation or deletion of MTSPs causes severe hereditary disease in humans (17), neuronal disorders, developmental problems and subfertility in mouse models (18-23). Although MTSPs share a conserved AAA domain, their other regions are entirely different, so they localize distinctly and function cooperatively but also individually (13).

The mechanism of cell division, either mitosis or meiosis, is a core issue in the study of the cell cycle. Abnormal cell division can cause aneuploidy, cancer cell-like features or infertile gametes. In normal meiosis, especially in female meiosis, gene stability is critical, and meiotic abnormalities are closely related to many human genetic diseases (3,24-26). Compared to mitosis, meiosis is a more unique process.

---

*Correspondence to:* Mr. Jin-Wei Liu, Department of Gynecology, Zhejiang Provincial People's Hospital, People's Hospital of Hangzhou Medical College, 158 Shangtang Road, Xiacheng, Hangzhou, Zhejiang 310014, P.R. China  
E-mail: zjulw@163.com

**Key words:** microtubule-severing proteins, katanin p60 ATPase-containing subunit A-like 1, oocytes, meiosis, spindle

Oocytes and spermatocytes do not have a typical centrosome, but some key centrosome components are found at the spindle poles and are essential for the organization of meiotic spindle poles. The division apparatus (regardless of the fact that its function is not limited to division), the spindle, is constructed from dynamic microtubules and all types of MAPs including MTSPs. Katanin p60 ATPase-containing subunit A-like 1 (p60 katanin-like 1) is an MTSP that exhibits typical microtubule-severing activity, and a study revealed that p60 katanin-like 1 is essential to maintain normal microtubule intensity at the poles of mitotic somatic cells (27). Additionally, p60 katanin-like 1 was revealed to regulate terminal dendrite stability and dendrite pruning in sensory neurons, and missense mutations caused intellectual disability and microcephaly in humans and defects in neuronal migration and morphology (18,19,21). However, no studies have been performed on the function of p60 katanin-like 1 in mammalian female meiosis. In the present study, it was revealed that p60 katanin-like 1, a member of the MTSP family, was predominantly enriched within oocytes and ovaries and essential for oocyte meiosis and maturation.

## Materials and methods

*General chemicals, reagents cells and animals.* Chemicals and reagents were obtained from Sigma-Aldrich; Merck KGaA unless otherwise stated. The NIH3T3 cell line was purchased from the American Type Culture Collection. A total of 265 3 week old female specific pathogen free ICR mice (weighing 18-20 g) used in this study were obtained from Vital River Experimental Animal Technical Co., Ltd. Animals were housed at a temperature of 20-26°C and a humidity of 40-70% with a 12 h light/dark cycle. The mice were fed in feeding boxes, food was replaced 2 times a week and the water bottle was replaced 3 times a week. All animal experiments were approved by the Animal Care and Use Committee of Nanjing Medical University (Nanjing, China) and were performed in accordance with institutional guidelines.

*Antibodies.* Mouse monoclonal anti- $\beta$ -actin (cat. no. A5316-100) antibody was obtained from Sigma-Aldrich; Merck KGaA. Mouse monoclonal anti-katanin p60 AL1 (A-10) (cat. no. sc-373814) and mouse monoclonal anti- $\beta$ -tubulin (cat. no. sc-5274) antibodies were purchased from Santa Cruz Biotechnology, Inc. Human anti-centromere CREST antibody (cat. no. 15-234) was purchased from Antibodies Incorporated. Mouse monoclonal anti-EGFP (F56-6A1.2.3) (cat. no. ab184601) was purchased from Abcam. Cy2-conjugated donkey anti-mouse IgG (code no. 715-225-150), rhodamine (TRITC)-conjugated donkey anti-goat IgG (code no. 705-025-147), and Alexa Fluor 647-conjugated donkey anti-human IgG (code no. 709-605-149) were purchased from Jackson ImmunoResearch Laboratories, Inc. Horseradish peroxidase (HRP)-conjugated rabbit anti-goat IgG (cat. no. 31402) and HRP-conjugated goat anti-mouse IgG (cat. no. 31430) were purchased from Invitrogen; Thermo Fisher Scientific, Inc.

*Oocyte collection and culture.* Immature oocytes arrested in prophase I [germinal vesicle (GV) oocytes] were obtained

from the ovaries of 3 to 4-week-old female ICR mice. The mice were first euthanized with CO<sub>2</sub> and then sacrificed by cervical dislocation, and the ovaries were isolated and placed in operation medium (HEPES) with 2.5 nM milrinone and 10% fetal bovine serum (FBS) (Gibco; Thermo Fisher Scientific, Inc.). Oocytes were released from the ovary by puncturing the follicles with a hypodermic needle. Cumulus cells were washed off the cumulus-oocyte complexes, and 50 isolated denuded oocytes were placed in 100- $\mu$ l droplets of culture medium under mineral oil in plastic dishes (BD Biosciences). The culture medium was MEM+ (MEM with 0.01 mM EDTA, 0.23 mM Na-pyruvate, 0.2 mM pen/strep, 3 mg/ml BSA and 20% FBS). The oocytes were cultured at 37.0°C, 5% O<sub>2</sub>, and 5% CO<sub>2</sub> in a humidified atmosphere. Prior to *in vitro* maturation (IVM), all culture medium included 2.5 nM milrinone to prevent the resumption of meiosis.

*siRNA production and transfection.* Sequences of all DNA templates used for siRNA production are listed in Table I. The sequence of the control templates was a mock sequence that did not specifically bind to any mRNA from the mouse genome. DNA templates against four different DNA coding (sequence coding for the amino acids in a protein, CDS) regions of KATNAL1 siRNA were designed online through BLOCK-iT™ RNAi Designer (<http://rnaidesigner.invitrogen.com/rnaiexpress/>) with some modifications. The sequence specificity was verified through a BLAST (<http://blast.ncbi.nlm.nih.gov/Blast.cgi>) homology search.

siRNAs were produced using the T7 RiboMAX™ Express RNAi System (Promega Corporation), according to the manufacturer's instructions. Briefly, for each double-stranded siRNA against one of the four KATNAL1 CDS regions, two pairs of synthesized complementary single-stranded DNA oligonucleotides were first annealed to form two double-stranded DNA templates. Subsequently, two complementary single-stranded siRNAs were separately synthesized in accordance with these two templates and then annealed to form a final double-stranded siRNA. Next, the siRNA was purified by conventional phenol/chloroform/isopropanol precipitation and then aliquoted and stored at -80°C after a quality check on an agarose gel. A ready-to-use siRNA mixture was prepared by mixing the siRNAs against four target regions together at an equal molar ratio to a final concentration of 5  $\mu$ M.

For siRNA transfection, the N-TERM™ Nanoparticle siRNA Transfection System (Sigma-Aldrich; Merck KGaA) was used. Briefly, two tubes, one containing 1.1  $\mu$ l N-TERM nanoparticles in 5.15  $\mu$ l nuclease-free water (Acros Organics) and the other containing 1.625  $\mu$ l of the siRNA mixture (5  $\mu$ M) in 4.625  $\mu$ l of siRNA dilution buffer (provided by the kit) were prepared; they were then gently mixed and incubated at room temperature (RT) for 20 min. Next, the siRNA-nanoparticle complex solution was added into a 100- $\mu$ l drop of medium containing 50 oocytes. After treatment for 12-14 h, the oocytes were washed to remove the nanoparticle-containing medium. After a period of 1-2 h, another round or two rounds of siRNA treatment were performed, depending on how difficult the target was to significantly knock down. During the whole siRNA treatment, which was typically 36-44 h long, 2.5 nM milrinone was included to prevent the resumption of meiosis. Next, the oocytes were transferred into milrinone-free MEM+

Table I. DNA oligos for siRNA production.

Target site	DNA templates
KATNAL1 CDS 58-76 <sup>a</sup>	Oligo1: <u>GGATCCTAATACGACTCACTATAGGAAGAATATGAACAGGTT</u> <sup>b</sup> Oligo2: <u>AAAACCTGTTTCATATTCTTCTATAGTGAGTCGTATTAGGATCC</u> <sup>b</sup> Oligo3: <u>GGATCCTAATACGACTCACTATAAACCTGTTTCATATTCTTCC</u> <sup>b</sup> Oligo4: <u>AAGGAAGAATATGAACAGGTTTATAGTGAGTCGTATTAGGATCC</u> <sup>b</sup>
KATNAL1 CDS 581-599 <sup>a</sup>	Oligo1: <u>GGATCCTAATACGACTCACTATAGGGACATTGTGTCCAGGAA</u> <sup>b</sup> Oligo2: <u>AATTCCTGGACACAATGTCCCTATAGTGAGTCGTATTAGGATCC</u> <sup>b</sup> Oligo3: <u>GGATCCTAATACGACTCACTATATTCCTGGACACAATGTCCC</u> <sup>b</sup> Oligo4: <u>AAGGGACATTGTGTCCAGGAATATAGTGAGTCGTATTAGGATCC</u> <sup>b</sup>
KATNAL1 CDS 701-719 <sup>a</sup>	Oligo1: <u>GGATCCTAATACGACTCACTATAGGATTAGAAGGCCATGGAA</u> <sup>b</sup> Oligo2: <u>AATTCATGGCCTTCTAATCCTATAGTGAGTCGTATTAGGATCC</u> <sup>b</sup> Oligo3: <u>GGATCCTAATACGACTCACTATATTCATGGCCTTCTAATCC</u> <sup>b</sup> Oligo4: <u>AAGGATTAGAAGGCCATGGAATATAGTGAGTCGTATTAGGATCC</u> <sup>b</sup>
KATNAL1 CDS 922-940 <sup>a</sup>	Oligo1: <u>GGATCCTAATACGACTCACTATAGATTCTATCTGCAGTCGAA</u> <sup>b</sup> Oligo2: <u>AATTCGACTGCAGATAGAATCTATAGTGAGTCGTATTAGGATCC</u> <sup>b</sup> Oligo3: <u>GGATCCTAATACGACTCACTATATTCGACTGCAGATAGAATC</u> <sup>b</sup> Oligo4: <u>AAGATTCTATCTGCAGTCGAATATAGTGAGTCGTATTAGGATCC</u> <sup>b</sup>
Control <sup>c</sup>	Oligo1: <u>GGATCCTAATACGACTCACTATACCTACGCCACCAATTCGTTT</u> <sup>b</sup> Oligo2: <u>AAAAACGAAATTGGTGGCGTAGGTATAGTGAGTCGTATTAGGATCC</u> <sup>b</sup> Oligo3: <u>GGATCCTAATACGACTCACTATAAACGAAATTGGTGGCGTAGG</u> <sup>b</sup> Oligo4: <u>AACCTACGCCACCAATTCGTTTTATAGTGAGTCGTATTAGGATCC</u> <sup>b</sup>

<sup>a</sup>The numbers are the starting and ending position of the target sites in KATNAL1 CDS (NM\_001033429.2 in NCBI). <sup>b</sup>Two pairs of DNA oligos are required for each double-strand siRNA. Oligo 2 is complementary with oligo 1 except for an 'AA' overhang at 5'; Oligo 3 is complementary with oligo 4 except for an 'AA' overhang at 5'. In each oligo, gene-specific sequences are underlined, other sequences are for recognition and binding by T7 RNA polymerase. <sup>c</sup>Control siRNA does not target to any mRNA sequence in mouse.

and cultured for 8 or 16 h. They were then used for the phenotype analysis experiment described below.

**Plasmid construction and mRNA synthesis.** Total RNA was extracted from 100 mouse oocytes using an Arcturus PicoPure RNA Isolation kit (Applied Biosystems; Thermo Fisher Scientific, Inc.), and cDNA was generated with a QIAquick PCR Purification kit (Qiagen GmbH). The following primers were used to amplify the CDS sequence of KATNAL1: Forward primer, 5'-CGCGGATCCGCCACCATGAATTTGGCGGAGATTTGTG-3' and reverse primer, 5'-AAGGAAAAAGCGGCCGCTCATGCAGACCCAACTCAAC-3'. The PCR products were purified, digested with *Bam*HI and *Not*I (New England Biolabs, Inc.), and then cloned into the pCS2<sup>+</sup> vector with EGFP tags.

To synthesize EGFP-KATNAL1 mRNA, the KATNAL1-pCS2<sup>+</sup> plasmids were linearized using *Eco*RI. Capped cRNAs were produced using *in vitro* transcription with an SP6 mMessage mMachine kit (Ambion; Thermo Fisher Scientific, Inc.) according to the manufacturer's instructions and then purified by an RNeasy Micro kit (Qiagen GmbH). The synthesized RNA was portioned into aliquots and stored at -80°C.

Microinjections of mRNA with a Narishige microinjector (Narishige Group) were used to knock down or overexpress specific proteins in mouse oocytes. Ten picoliters of the mRNA solution (10 ng/ml) was injected into the oocyte cytoplasm for

overexpression analysis. The same amount of RNase-free PBS was injected as a control.

After the injections, the oocytes were arrested at the GV stage in M2 medium containing 2.5 mM milrinone for 20 h to either facilitate the knockdown of mRNA translation or permit overexpression. Following three washes, the oocytes were cultured in milrinone-free medium for different time-points to evaluate the cellular events during maturation.

**Immunofluorescence.** The oocytes were briefly washed in PBS with 0.05% polyvinylpyrrolidone (PVP), permeated in 0.5% Triton X-100/PHEM (60 mM PIPES, 25 mM HEPES pH 6.9, 10 mM EGTA, 8 mM MgSO<sub>4</sub>) for 5 min and washed three times rapidly in PBS/PVP. Next, the oocytes were fixed in 3.7% paraformaldehyde (PFA)/PHEM for 20 min at room temperature, washed three times (10 min each) in PBS/PVP and blocked with blocking buffer (1% BSA/PHEM with 100 mM glycine) at room temperature for 1 h. Then, the oocytes were in sequence incubated at 4°C overnight with a primary antibody diluted in blocking buffer, washed three times (10 min each) in PBS with 0.05% Tween-20 (PBST), incubated at room temperature for 45 min with a secondary antibody diluted in blocking buffer (1:750 in all cases), and washed three times (10 min each) in PBST. Finally, the DNA was stained with 10 µg/ml Hoechst 33258 (Sigma-Aldrich; Merck KGaA) at room temperature for 10 min, and the oocytes were mounted onto a slide with mounting medium (0.5% propyl gallate, 0.1 M

Tris-HCl, pH 7.4, 88% glycerol) and covered with a cover glass (thickness, 0.13–0.17  $\mu\text{m}$ ). To maintain the dimension of the oocytes, two strips of double-stick tape (thickness, 90  $\mu\text{m}$ ) were placed between the slide and cover glass. The primary antibodies were diluted as follows: Anti-p60 katanin-like 1, 1:200; anti-tubulin, 1:500; anti-human centromere, 1:500. The oocytes were examined with an Andor Revolution spinning disk confocal workstation (Oxford instruments).

**Western blotting.** A total of 100 oocytes were lysed in Laemmli sample buffer (Bio-Rad Laboratories, Inc.) containing a protease inhibitor and boiled for 5 min before being subjected to 10% SDS-PAGE. The separated proteins were transferred to a PVDF membrane and then blocked in TBST (TBS containing 0.05% Tween-20) with 5% nonfat milk at room temperature for 1 h. Then, the PVDF membrane was separated and incubated overnight at 4°C with primary antibodies as follows: Mouse monoclonal anti- $\beta$ -actin (cat. no. A5316-100) was diluted with a blocking buffer (TBS containing 0.05% Tween-20) at a ratio of 1:1,000; mouse monoclonal anti-katanin p60 AL1 (A-10) (cat. no. sc-373814; Santa Cruz Biotechnology, Inc.) was diluted with a blocking buffer at a ratio of 1:500; mouse monoclonal anti- $\gamma$ -tubulin (cat. no. T3559-.2ML; Sigma-Aldrich; Merck KGaA) was diluted with a blocking buffer at a ratio of 1:2,000. After being washed in TBST, the membranes were incubated with HRP-conjugated rabbit anti-goat IgG or HRP-conjugated goat anti-mouse IgG (diluted with a blocking buffer to 1:1,000) for 1 h at room temperature and then processed using an ECL Plus Western Blotting Detection System (Vazyme). ImageJ 1.8.0 (National Institutes of Health) was used for data analysis.

**Immunoprecipitation.** For immunoprecipitation experiments, 5  $\mu\text{g}$  control IgG or anti-p60 katanin-like 1 antibody was first coupled to 30  $\mu\text{l}$  protein-A/G beads [M&C Gene Technology (Beijing), Ltd] for 4 h at 4°C on a rotating wheel in 250  $\mu\text{l}$  IP buffer (20 mM Tris-HCl, pH 8.0, 10 mM EDTA, 1 mM EGTA, 150 mM NaCl, 0.05% Triton X-100, 0.05% Nonidet P-40, and 1 mM phenylmethylsulfonyl fluoride) with 1:100 protease inhibitor and 1:500 phosphatase inhibitor (both from Sigma-Aldrich; Merck KGaA). Meanwhile, 600 ZP-free GV oocytes were lysed and ultrasonicated in 250 IP buffer before being incubated with 30  $\mu\text{l}$  protein-A/G beads for 4 h at 4°C. Then, a protein A/G-coupled control IgG or anti-p60 katanin-like 1 antibody was incubated overnight at 4°C with 250  $\mu\text{l}$  pre-cleaned oocyte lysate supernatant. Finally, the beads were washed the next morning three times for 10 min each with 1 ml IP buffer, and the resulting beads with bound immunocomplexes were subjected to 10% SDS-PAGE and silver staining by incubating with 0.1% AgNO<sub>3</sub> solution at room temperature for 30 min.

**Mitochondrial staining.** For mitochondrial staining, the oocytes were stained in HEPES containing 100 nM MitoTracker (cat. no. M7521; Invitrogen; Thermo Fisher Scientific, Inc.) and 10  $\mu\text{g}/\text{ml}$  Hoechst 33342 (Sigma-Aldrich; Merck KGaA) for 30 min. Subsequently, the oocytes were examined with an Andor Revolution spin disk confocal workstation.

**Data analysis and statistics.** All experiments were repeated at least three times. Measurements on confocal images was performed with ImageJ (National Institutes of Health). Data

are presented as the average  $\pm$  sem. Statistical comparisons were performed with Student's t-test in Excel.  $P < 0.05$  was considered to indicate a statistically significant difference.

## Results and Discussion

*p60 katanin-like 1 is predominant in mouse ovaries and oocytes.* The expression and localization patterns of p60 katanin-like 1 were first examined in mouse ovaries and oocytes. Western blot analysis revealed that the expression of KATNAL1 in oocytes was significantly higher than that in somatic cells (Fig. 1A), indicating that p60 katanin-like 1 may be more critical in oocytes. p60 katanin-like 1 was more pronounced in oocytes than in granular cells (Fig. 1B), indicating that the role of p60 katanin-like 1 may be primarily in oocytes. Additionally, it was also determined that the abundance of p60 katanin-like 1 in the ovary and testis was markedly high (Fig. 1C), indicating that p60 katanin-like 1 may be closely related to the activities of germ cells.

*p60 katanin-like 1 is located at the spindle poles of MI and MII oocytes and co-localizes with  $\gamma$ -tubulin.* The abundance of p60 katanin-like 1 in mouse oocytes indicated that p60 katanin-like 1 participates in germ cell activity. Next, the localization of p60 katanin-like 1 in oocytes was assessed by immunofluorescence. p60 katanin-like 1 was located at the spindle poles of MI and MII mouse oocytes (Fig. 2A and B). In addition, p60 katanin-like 1 and  $\gamma$ -tubulin co-localized at the spindle poles of MI and MII oocytes (Fig. 2C), indicating that the function of p60 katanin-like 1 may be related to the organization of spindle poles.

*p60 katanin-like 1 knockdown leads to severe maturation abnormalities in oocytes.* To explore the function of p60 katanin-like 1 in oocyte development, specific siRNAs for p60 katanin-like 1 were designed and the siRNA mixture was transfected into GV oocytes with nanoparticle reagent. Then, the effect of siRNA knockdown was examined. RT-PCR (Fig. 3B, lower panel) and western blot (Fig. 3A) revealed that siRNA knockdown reduced the p60 katanin-like 1 mRNA or protein level to 20% of that in the control. RT-PCR also revealed that the siRNAs could specifically target p60 katanin-like 1 but had no detectable effect on p60 katanin, another member of MTSP family (Fig. 3B, upper panel). Next, oocyte maturation after p60 katanin-like 1 knockdown was examined. Compared with that in the control, p60 katanin-like 1-depleted cells did not exhibit a significantly lower rate of germinal vesicle breakdown (GVBD) after 3 h of *in vitro* maturation (IVM) (Fig. 3C upper panel). However, the percentage of cells exhibiting a first polar body (1 Pb) extrusion was significantly lower than that of the control group after 16 h of IVM (Fig. 3C, lower panel). Furthermore, *in vitro* fertilization (IVF) with normal sperm revealed that the p60 katanin-like 1-depleted group had a decreased fertility rate and significantly more fertilized eggs with multiple pronuclei (less fertilized eggs with two pronuclei) than the control group (Fig. 3D). These results indicated that p60 katanin-like 1 is essential for the potential of oocytes.

*p60 katanin-like 1 knockdown causes abnormal pole-correlated spindle organization in metaphase I (MI) or metaphase II (MII)*

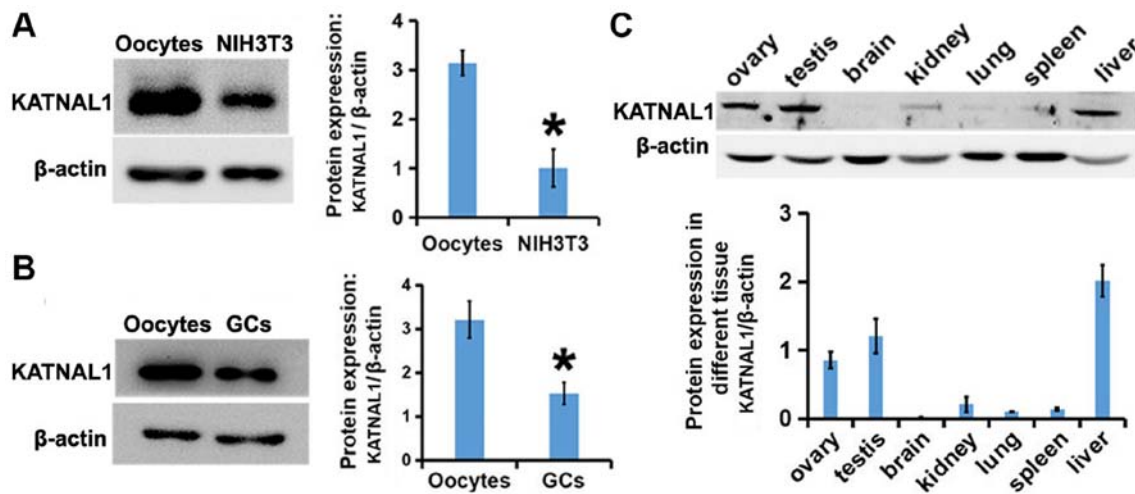


Figure 1. KATNAL1 is predominant in mouse ovaries and oocytes. (A and B) Western blotting revealed that there was significantly more KATNAL1 in oocytes than in (A) somatic cells or (B) granular cells. (C) Western blot quantification revealed that KATNAL1 was more enriched in the ovaries and testes than in other tissues.  $\beta$ -actin was used as a control. \* $P < 0.05$  is considered to indicate statistically significant differences.

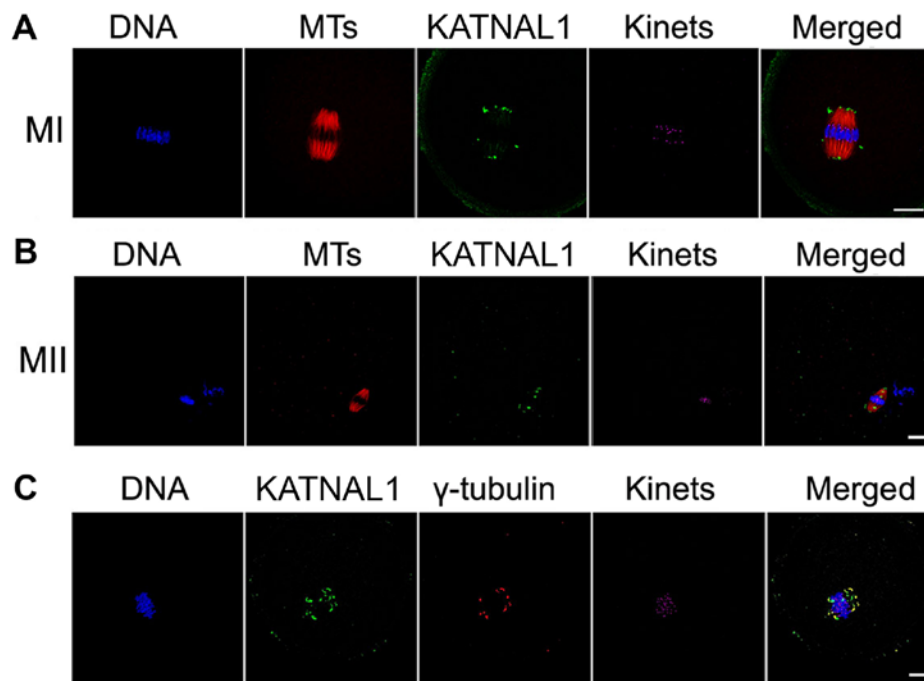


Figure 2. KATNAL1 is located at the spindle poles of MI and MII oocytes and co-localizes with  $\gamma$ -tubulin. (A and B) Immunofluorescence revealed that KATNAL1 was located at the spindle poles of (A) MI and (B) MII mouse oocytes. Tubulin is displayed in red, KATNAL1 in green, kinetochores in magenta, and DNA in blue. (C) At the MI stage, KATNAL1 co-localized with  $\gamma$ -tubulin at the spindle poles. DNA is displayed in blue, KATNAL1 in green,  $\gamma$ -tubulin in red, and the kinetochores in magenta. Scale bar, 20  $\mu$ m.

*oocytes*. Next, the spindle phenotype was characterized after p60 katanin-like 1 knockdown. p60 katanin-like 1 knockdown caused different extents of spindle irregularities. The ratio of width:length of the spindles was assessed and it was revealed that, compared with the control, the spindles in the p60 katanin-like 1-knockdown group were longer and thinner (Fig. 4A). In addition, p60 katanin-like 1 knockdown resulted in more aster-like microtubule structures in the cytoplasm and more multipolar spindles than control cells (Fig. 4B). Since p60 katanin-like 1 was concentrated at the spindle poles and these phenotypes were pole-related, we next examined whether p60 katanin-like 1 interacts with crucial pole components. Co-immunoprecipitation

experiments revealed that p60 katanin-like 1 and  $\gamma$ -tubulin interacted well with each other (Fig. 4C). Collectively, these results revealed that p60 katanin-like 1 may interact with  $\gamma$ -tubulin and that p60 katanin-like 1 knockdown caused pole-correlated spindle defects.

In addition, EGFP-KATNAL1 mRNA was expressed *in vitro* and injected into oocytes, which inhibited development. After 8 h of development *in vitro*, immunofluorescence of the EGFP tags was performed and it was revealed that the localization of the EGFP tags was consistent with that of p60 katanin-like 1 in the oocytes, which demonstrated the expression of EGFP-KATNAL1 mRNA in oocytes (Fig. S1A).

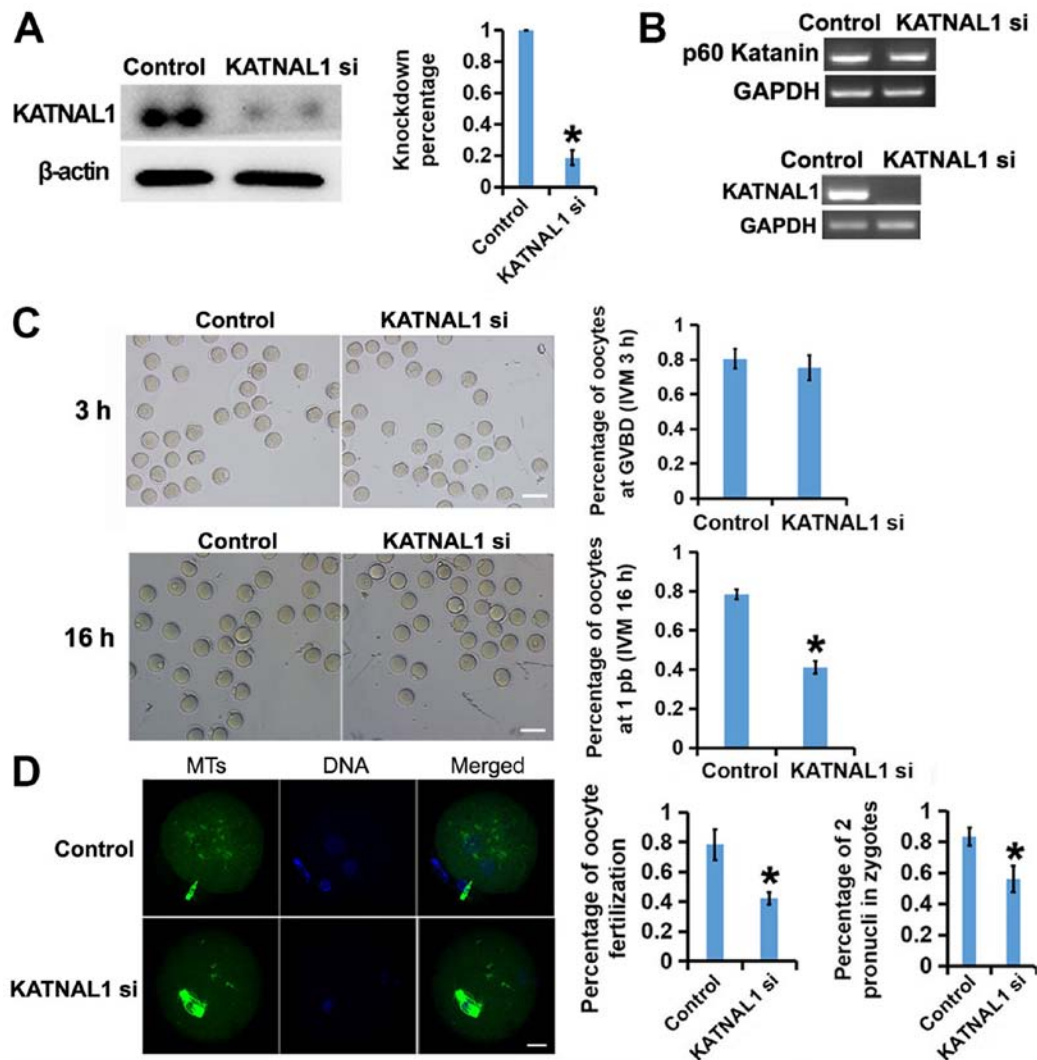


Figure 3. KATNAL1 knockdown leads to severe maturation abnormalities in oocytes. (A) Western blotting revealed that KATNAL1 was efficiently knocked down by specific siRNA.  $\beta$ -actin was used as a control. (B) RT-PCR revealed that siRNA specifically reduced KATNAL1 mRNA levels but did not affect p60 katanin, another member of the MTSP family. GAPDH was used as a control. (C) After 3 h of IVM, there was no significant difference in the percentage of GVBD oocytes between the KATNAL1-knockdown and control groups. After 16 h of IVM, there was a significant difference in the percentage of 1 Pb (first polar body) oocytes between the KATNAL1-knockdown and control groups. Scale bar, 100  $\mu$ m. (D) IVF revealed that KATNAL1 depletion induced a significant decrease in the fertility rate and the 2-PN (pronuclei) rate. DNA is displayed in blue, tubulin in green. Scale bar, 20  $\mu$ m. \* $P$ <0.05 is considered to indicate statistically significant differences. IVF, *in vitro* fertilization.

In addition, it was revealed that oocytes overexpressing KATNAL1 had a wide spindle shape at the two poles (Fig. S1B). After 16 h of *in vitro* development, 1 Pb extrusion in oocytes decreased significantly compared to that in control cells (Fig. S1C). It was speculated that the overexpression of KATNAL1 may lead to disorder in the polar structure of the spindle by severing the microtubules excessively, thus affecting the morphology and function of the spindle, thereby affecting oocyte development.

*p60 katanin-like 1 knockdown causes the abnormal subcellular distribution of mitochondria in oocytes.* To further study how p60 katanin-like 1 knockdown caused severe defects in oocyte maturation and spindle organization, its effects on the mitochondria were investigated in oocytes. The deletion of *KATNAL1* resulted in an uneven distribution of mitochondria in oocytes compared with their distribution in the control group (Fig. 5A). Through careful assessment of the

mitochondrial intensity in each subregion, it was determined that the mitochondria in the KATNAL1-depleted oocytes tended to gather in the center; accordingly, there were fewer mitochondria near the membrane (Fig. 5B). These results indicate that KATNAL1 knockdown markedly affected the distribution of mitochondria.

Normal meiosis ensures the euploidy of oocytes, subsequent regular fertilization, and early embryo development until the birth of healthy pups. Meiotic spindles undergo marked changes throughout meiosis, and markedly abnormal organization of the spindle microtubules frequently causes defective meiosis, consequently affecting all the following processes (3,16,22-26). Typical abnormal spindle organization includes improper kinetochore-MT attachment (merotelic, syntelic), spindles with significantly decreased MT intensity, an abnormal width:length ratio (which usually indicates that MT dynamics are abnormal), a monopolar spindle, and an extra aster-like microtubule structure. In the present study,

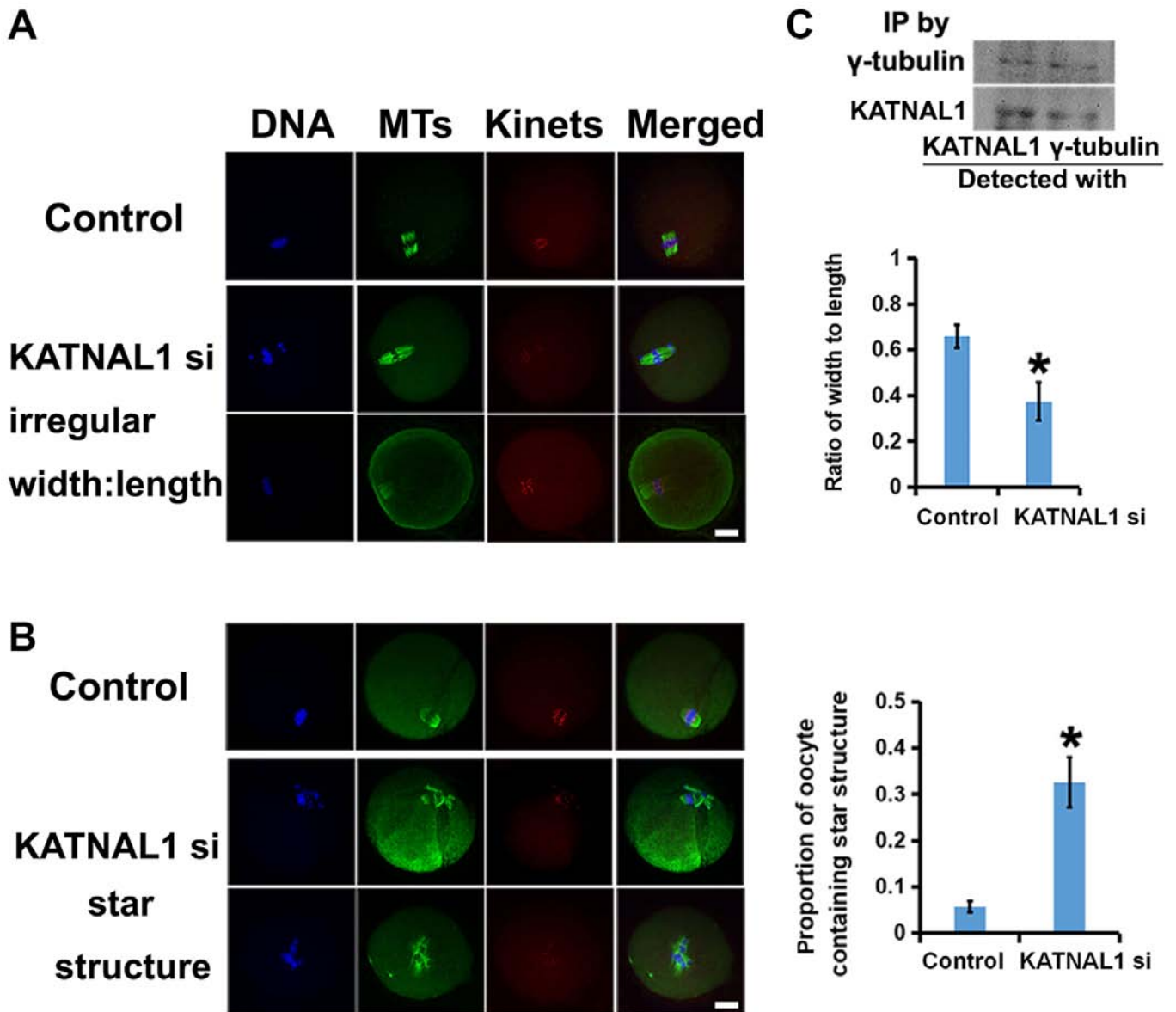


Figure 4. KATNAL1 knockdown causes abnormal pole-correlated spindle organization in MI or MII oocytes. (A) In MI-stage oocytes, KATNAL1 knockdown produced longer and thinner spindles than those in the control cells. The measurement of the spindle width:length was significantly decreased. Tubulin is displayed in green, kinetochores in red, and DNA in blue. Scale bar, 20  $\mu$ m. (B) KATNAL1 knockdown resulted in multipolar spindles (middle) or extra aster microtubules (bottom) within the cytoplasm of oocytes. Tubulin is displayed in green, kinetochores in red, and DNA in blue. Scale bar, 20  $\mu$ m. (C) Co-IP revealed that p60 katanin-like 1 and  $\gamma$ -tubulin precipitated with each other. \* $P < 0.05$  is considered to indicate statistically significant differences.

it was first revealed that p60 katanin-like 1, a member of the MTSP family, is predominant in the ovaries and more enriched in oocytes than granular cells, indicating that p60 katanin-like 1 may play essential roles in oocyte growth and maturation. It was revealed in the present study, that p60 katanin-like 1 localizes at the spindle poles and interacts with  $\gamma$ -tubulin, indicating that the function of p60 katanin-like 1 may be correlated with the organization of the spindle poles. Next, p60 katanin-like 1 was depleted with specific siRNAs and mainly three typical meiotic spindle phenotypes were revealed: An abnormal width:length ratio, multipolar microtubules, and an extra aster-like microtubule structure. Previous

studies revealed that the depletion of the spindle pole matrix caused an abnormal width:length ratio, multipolarity or additional asters when diverse centrosome or pole components were knocked down or depleted (28-32). These results mostly correspond with the results of our study, suggesting that p60 katanin-like 1 is essential for meiotic spindle integrity by regulating pole organization. A previous study reported that in U2OS cells, p60 katanin-like 1 was restricted to the spindle poles and absent from centrosomes, and the siRNA depletion of p60 katanin-like 1 from U2OS cells caused a significant reduction in the density of the spindle poles and increased the spindle length (27). Thus, p60 katanin-like 1 functions

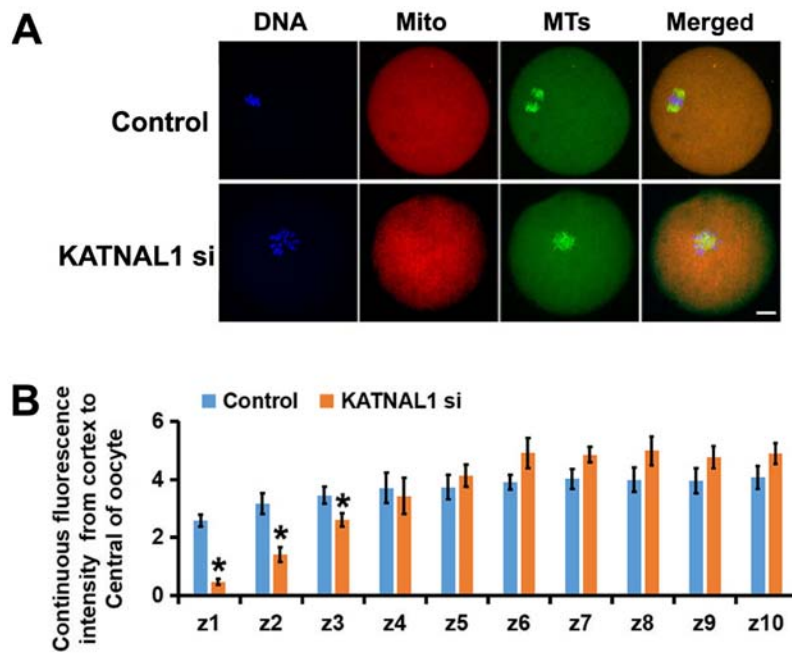


Figure 5. KATNAL1 knockdown causes the abnormal subcellular distribution of mitochondria in oocytes. (A) Immunofluorescence revealed abnormal mitochondrial aggregation after KATNAL1 knockdown. DNA is displayed in blue, tubulin in green, mitochondria in red. Scale bar, 20  $\mu\text{m}$ . (B) The continuous measurement of the mitochondrial intensity revealed that the mitochondrial intensity was significantly decreased near the membrane while increased near the center. \* $P < 0.05$  is considered to indicate statistically significant differences.

somewhat similarly in meiosis and mitosis. However, it was also observed that p60 katanin-like 1 depletion caused multipolar spindles and extra asters, which could cause even severe meiotic defects. Therefore, it appears that p60 katanin-like 1 is more indispensable in meiosis than in mitosis. Numerous studies have demonstrated that defective spindle organization could severely affect the progression of meiosis and subsequent fertilization. In the present study, p60 katanin-like 1 knockdown significantly reduced the percentage of GVBD or MII oocytes, which further indicates its essential roles in meiosis.

Mitochondria are the factory for adenosine triphosphate (ATP) generation, and the abnormal subcellular distribution of mitochondria could lead to insufficient ATP generation in some regions and excessive ATP generation in others; either situation is unfavorable for normal meiosis since the regular cell cycle, either mitosis or meiosis, requires the cooperation of multiple enzymes that bind and hydrolyze the proper level of ATP to perform appropriately. Insufficient or excessive ATP generation could have an inhibitory or activating effect that could inhibit or overactivate these enzymes. In fact, multiple previous studies revealed that abnormal mitochondrial distribution caused significantly reduced cellular ATP levels (33-36). Mitochondrial malfunction is closely related to a reduction in reproductivity (37-40). Mitochondria are also highly dynamic and motile during the cell cycle, and their movement is microtubule-dependent (41-44); therefore, the abnormal mitochondrial distribution in our study could be caused by irregular spindle organization. This eventually disrupted spindle organization and caused the uneven distribution of mitochondria, which were both caused by p60 katanin-like 1 knockdown; together, these retarded meiosis and reduced fertilization.

In conclusion, the present study, revealed for the first time that p60 katanin-like 1, an MTSP that is enriched in oocytes, is concentrated at the spindle poles and essential for pole organization during mouse oocyte meiosis. p60 katanin-like 1 knockdown caused severe spindle defects characterized by an abnormal width:length ratio, multipolarity, and extra aster microtubules. p60 katanin-like 1 knockdown also caused irregular mitochondrial distribution. These factors collectively retarded meiosis and reduced fertilization. Further investigation is required to determine how p60 katanin-like 1 organizes the spindle poles and what regulates its activity.

#### Acknowledgements

The authors would like to thank Dr Zhang (Hangzhou Medical College) for providing us with a mitochondrial probe.

#### Funding

This present study was supported by the Grant for Zhejiang Provincial Science and Technology Department and the Department of Health (2017KY199 and 2018KY240).

#### Availability of data and materials

The datasets used and/or analyzed during the current study are available from the corresponding author on reasonable request.

#### Authors' contributions

JWL and LLG conceived and designed the experiments. LLG, FX, ZJ and XYY performed the experiments. LLG analyzed the data. JWL and LLG contributed the reagents/materials/analysis

tools. JWJ and LLG wrote the paper. All authors read and approved the manuscript and agree to be accountable for all aspects of the research in ensuring that the accuracy or integrity of any part of the work are appropriately investigated and resolved.

### Ethics approval and consent to participate

All animal experiments were approved by the Animal Care and Use Committee of Nanjing Medical University (Nanjing, China) and performed in accordance with institutional guidelines.

### Patient consent for publication

Not applicable.

### Competing interests

The authors declare that they have no competing interests.

### References

- Sferra A, Fattori F, Rizza T, Flex E, Bellacchio E, Bruselles A, Petrini S, Cecchetti S, Teson M, Restaldi F, *et al*: Defective kinesin binding of TUBB2A causes progressive spastic ataxia syndrome resembling saccinopathy. *Hum Mol Genet* 27: 1892-1904, 2018.
- Luscan R, Mechaussier S, Paul A, Tian G, Gerard X, Defoort-Dellhemmes S, Loundon N, Audo I, Bonnin S, LeGargasson JF, *et al*: Mutations in TUBB4B cause a distinctive sensorineural disease. *Am J Hum Genet* 101: 1006-1012, 2017.
- Feng R, Sang Q, Kuang Y, Sun X, Yan Z, Zhang S, Shi J, Tian G, Luchniak A, Fukuda Y, *et al*: Mutations in TUBB8 and human oocyte meiotic arrest. *N Engl J Med* 374: 223-232, 2016.
- Martin M and Akhmanova A: Coming into focus: Mechanisms of microtubule minus-end organization. *Trends Cell Biol* 28: 574-588, 2018.
- Aher A and Akhmanova A: Tipping microtubule dynamics, one protofilament at a time. *Curr Opin Cell Biol* 50: 86-93, 2018.
- Akhmanova A and Steinmetz MO: Control of microtubule organization and dynamics: Two ends in the limelight. *Nat Rev Mol Cell Biol* 16: 711-726, 2015.
- Huynh W and Vale RD: Disease-associated mutations in human BICD2 hyperactivate motility of dynein-dynactin. *J Cell Biol* 216: 3051-3060, 2017.
- Lewis WR, Malarkey EB, Tritschler D, Bower R, Pasek RC, Porath JD, Birket SE, Saunier S, Antignac C, Knowles MR, *et al*: Mutation of growth arrest specific 8 reveals a role in motile cilia function and human disease. *PLoS Genet* 12: e1006220, 2016.
- Decker JM, Kruger L, Sydow A, Dennissen FJ, Siskova Z, Mandelkow E and Mandelkow EM: The Tau/A152T mutation, a risk factor for frontotemporal-spectrum disorders, leads to NR2B receptor-mediated excitotoxicity. *EMBO Rep* 17: 552-569, 2016.
- Frickey T and Lupas AN: Phylogenetic analysis of AAA proteins. *J Struct Biol* 146: 2-10, 2004.
- Vale RD: AAA proteins. Lords of the ring. *J Cell Biol* 150: F13-E19, 2000.
- Buster D, McNally K and McNally FJ: Katanin inhibition prevents the redistribution of gamma-tubulin at mitosis. *J Cell Sci* 115: 1083-1092, 2002.
- Sharp DJ and Ross JL: Microtubule-severing enzymes at the cutting edge. *J Cell Sci* 125: 2561-2569, 2012.
- Zhang D, Rogers GC, Buster DW and Sharp DJ: Three microtubule severing enzymes contribute to the 'Pacman-flux' machinery that moves chromosomes. *J Cell Biol* 177: 231-242, 2007.
- Zhang D, Grode KD, Stewman SF, Diaz-Valencia JD, Liebling E, Rath U, Riera T, Currie JD, Buster DW, Asenjo AB, *et al*: *Drosophila* katanin is a microtubule depolymerase that regulates cortical-microtubule plus-end interactions and cell migration. *Nat Cell Biol* 13: 361-370, 2011.
- Srayko M, O'Toole ET, Hyman AA and Muller-Reichert T: Katanin disrupts the microtubule lattice and increases polymer number in *C. elegans* meiosis. *Curr Biol* 16: 1944-1949, 2006.
- Errico A, Ballabio A and Rugarli EI: Spastin, the protein mutated in autosomal dominant hereditary spastic paraplegia, is involved in microtubule dynamics. *Hum Mol Genet* 11: 153-163, 2002.
- Banks G, Lassi G, Hoerder-Suabedissen A, Tinarelli F, Simon MM, Wilcox A, Lau P, Lawson TN, Johnson S, Rutman A, *et al*: A missense mutation in *Katn1l* underlies behavioural, neurological and ciliary anomalies. *Mol Psychiatry* 23: 713-722, 2018.
- Mishra-Gorur K, Caglayan AO, Schaffer AE, Chabu C, Henegariu O, Vonhoff F, Akgumus GT, Nishimura S, Han W, Tu S, *et al*: Mutations in *KATNB1* cause complex cerebral malformations by disrupting asymmetrically dividing neural progenitors. *Neuron* 84: 1226-1239, 2014.
- Mao CX, Xiong Y, Xiong Z, Wang Q, Zhang YQ and Jin S: Microtubule-severing protein Katanin regulates neuromuscular junction development and dendritic elaboration in *Drosophila*. *Development* 141: 1064-1074, 2014.
- Stewart A, Tsubouchi A, Rolls MM, Tracey WD and Sherwood NT: Katanin p60-like promotes microtubule growth and terminal dendrite stability in the larval class IV sensory neurons of *Drosophila*. *J Neurosci* 32: 11631-11642, 2012.
- O'Donnell L, Rhodes D, Smith SJ, Merriner DJ, Clark BJ, Borg C, Whittle B, O'Connor AE, Smith LB, McNally FJ, *et al*: An essential role for katanin p80 and microtubule severing in male gamete production. *PLoS Genet* 8: e1002698, 2012.
- Smith LB, Milne L, Nelson N, Eddie S, Brown P, Atanassova N, O'Bryan MK, O'Donnell L, Rhodes D, Wells S, *et al*: *KATNAL1* regulation of sertoli cell microtubule dynamics is essential for spermiogenesis and male fertility. *PLoS Genet* 8: e1002697, 2012.
- Chen B, Zhang Z, Sun X, Kuang Y, Mao X, Wang X, Yan Z, Li B, Xu Y, Yu M, *et al*: Biallelic mutations in *PATL2* cause female infertility characterized by oocyte maturation arrest. *Am J Hum Genet* 101: 609-615, 2017.
- Nguyen AL, Marin D, Zhou A, Gentilello AS, Smoak EM, Cao Z, Fedick A, Wang Y, Taylor D, Scott RT Jr, *et al*: Identification and characterization of Aurora kinase B and C variants associated with maternal aneuploidy. *Mol Hum Reprod* 23: 406-416, 2017.
- Caburet S, Arboleda VA, Llano E, Overbeek PA, Barbero JL, Oka K, Harrison W, Vaiman D, Ben-Neriah Z, Garcia-Tuñon I, *et al*: Mutant cohesin in premature ovarian failure. *N Engl J Med* 370: 943-949, 2014.
- Sonbuchner TM, Rath U and Sharp DJ: *KL1* is a novel microtubule severing enzyme that regulates mitotic spindle architecture. *Cell Cycle* 9: 2403-2411, 2010.
- Pimenta-Marques A, Bento I, Lopes CA, Duarte P, Jana SC and Bettencourt-Dias M: A mechanism for the elimination of the female gamete centrosome in *Drosophila melanogaster*. *Science* 353: aaf4866, 2016.
- Connolly AA, Osterberg V, Christensen S, Price M, Lu C, Chicas-Cruz K, Lockery S, Mains PE and Bowerman B: *Caenorhabditis elegans* oocyte meiotic spindle pole assembly requires microtubule severing and the calponin homology domain protein *ASPM-1*. *Mol Biol Cell* 25: 1298-1311, 2014.
- Kim JS, Kim EJ, Oh JS, Park IC and Hwang SG: *CIP2A* modulates cell-cycle progression in human cancer cells by regulating the stability and activity of *Plk1*. *Cancer Res* 73: 6667-6678, 2013.
- Patel H, Zich J, Serrels B, Rickman C, Hardwick KG, Frame MC and Brunton VG: *Kindlin-1* regulates mitotic spindle formation by interacting with integrins and *Plk-1*. *Nat Commun* 4: 2056, 2013.
- Eot-Houllier G, Venoux M, Vidal-Eychenie S, Hoang MT, Giorgi D and Rouquier S: *Plk1* regulates both *ASAP* localization and its role in spindle pole integrity. *J Biol Chem* 285: 29556-29568, 2010.
- Zhou CX, Shi LY, Li RC, Liu YH, Xu BQ, Liu JW, Yuan B, Yang ZX, Ying XY and Zhang D: *GTPase-activating protein Elmod2* is essential for meiotic progression in mouse oocytes. *Cell Cycle* 16: 852-860, 2017.
- Zhang XL, Liu P, Yang ZX, Zhao JJ, Gao LL, Yuan B, Shi LY, Zhou CX, Qiao HF, Liu YH, *et al*: *Pnma5* is essential to the progression of meiosis in mouse oocytes through a chain of phosphorylation. *Oncotarget* 8: 96809-96825, 2017.
- Dinkelmann MV, Zhang H, Skop AR and White JG: *SPD-3* is required for spindle alignment in *Caenorhabditis elegans* embryos and localizes to mitochondria. *Genetics* 177: 1609-1620, 2007.

36. Kong XW, Wang DH, Zhou CJ, Zhou HX and Liang CG: Loss of function of KIF1B impairs oocyte meiotic maturation and early embryonic development in mice. *Mol Reprod Dev* 83: 1027-1040, 2016.
37. Maccarinelli F, Regoni M, Carmona F, Poli M, Meyron-Holtz EG and Arosio P: Mitochondrial ferritin deficiency reduces male fertility in mice. *Reprod Fertil Dev* 29: 2005-2010, 2017.
38. Wang M, Huang YP, Wu H, Song K, Wan C, Chi AN, Xiao YM and Zhao XY: Mitochondrial complex I deficiency leads to the retardation of early embryonic development in *Ndufs4* knockout mice. *Peer J* 5: e3339, 2017.
39. May-Panloup P, Boucret L, Chao de la Barca JM, Desquirit-Dumas V, Ferre-L'Hottelier V, Moriniere C, Descamps P, Procaccio V and Reynier P: Ovarian ageing: The role of mitochondria in oocytes and follicles. *Hum Reprod Update* 22: 725-743, 2016.
40. Ben-Meir A, Burstein E, Borrego-Alvarez A, Chong J, Wong E, Yavorska T, Naranian T, Chi M, Wang Y, Bentov Y, *et al*: Coenzyme Q10 restores oocyte mitochondrial function and fertility during reproductive aging. *Aging Cell* 14: 887-895, 2015.
41. Bartolak-Suki E, Imsirovic J, Nishibori Y, Krishnan R and Suki B: Regulation of mitochondrial structure and dynamics by the cytoskeleton and mechanical factors. *Int J Mol Sci* 18: pii: E1812, 2017.
42. Fu L, Dong Q, He J, Wang X, Xing J, Wang E, Qiu X and Li Q: SIRT4 inhibits malignancy progression of NSCLCs, through mitochondrial dynamics mediated by the ERK-Drp1 pathway. *Oncogene* 36: 2724-2736, 2017.
43. Wang C, Du W, Su QP, Zhu M, Feng P, Li Y, Zhou Y, Mi N, Zhu Y, Jiang D *et al*: Dynamic tubulation of mitochondria drives mitochondrial network formation. *Cell Res* 25: 1108-1120, 2015.
44. Fu C, Jain D, Costa J, Velve-Casquillas G and Tran PT: mmb1p binds mitochondria to dynamic microtubules. *Curr Biol* 21: 1431-1439, 2011.